Journal of Sustainable Forestry, 32:527–548, 2013

ISSN: 1054-9811 print/1540-756X online
DOI: 10.1080/10549811.2013.779198

Characterizing Spatial Distributions of Insect Pests Across Alaskan Forested Landscape: A Case Study Using Aspen Leaf Miner (*Phyllocnistis populiella* Chambers)

ROBIN M. REICH[1], JOHN E. LUNDQUIST[2], and VANESSA A. BRAVO[1]

[1]*Department of Forest and Rangeland Stewardship, Colorado State University, Fort Collins, Colorado, USA*

[2]*Region 10 Forest Health Protection and Pacific Northwest Research Station, USDA Forest Service, Anchorage, Alaska, USA*

*Insects are ectotherms that cannot regulate their own temperature, and thus rely on and are at the disposal of the surrounding environment. In this study, long-term climatic data are used to stratify forested regions of Alaska into climatic zones based on temperature and precipitation. Temperature and precipitation are shown to be important ecological drivers in determining the distribution of aspen leaf minor (*Phyllocnistis populiella *Chambers) and the aspen (*Populus tremuloides *Michx.) host in the state of Alaska. Climatic regions based on temperatures and precipitation accounted for 83 to 97% of the variability in the probability of observing aspen and the aspen leaf minor (ALM). The frequency of observing aspen was highest throughout the central region of the state, which represents a climate with low to moderate levels of precipitation and cold to mild temperatures. The highest probability of observing aspen was in the mild-very cold region of the state. The probability of observing ALM in a given climate zone followed a pattern similar to aspen. Differences were in the colder and drier climate zones where the probability of observing ALM decreased to near zero. The derived climatic models could be used to provide a basis for the analysis of climatic impacts on the distribution of forest insects throughout the state.*

Address correspondence to John E. Lundquist, Region 10 Forest Health Protection and Pacific Northwest Research Station, USDA Forest Service, 3301 'C' Street, Suite 202, Anchorage, AK 99503, USA. E-mail: jlundquist@fs.fed.us

KEYWORDS binary classification trees, climate, roadside surveys, satellite imagery, spatial error model

INTRODUCTION

The aspen leaf miner (*Phyllocnistis populiella* Chambers)—a moth native to North America and in the family Gracillariidae—is widespread, feeding on the epidermal leaf cells of quaking aspen (*Populus tremuloides* Michx.) and balsam poplar (*Populus balsamifera* L.). Because the cuticle remains intact, the crowns of infested trees commonly develop a striking silver gray cast (Condrashoff, 1964; Wagner, DeFoliart, Doak, & Schneiderheinze, 2008). Annual forest pest surveys conducted by the USDA Forest Service before 1999 found aspen leaf miner (ALM) to exist at endemic population levels in Alaska. Subsequently, however, populations increased steadily and now this defoliator is a conspicuous element on hundreds of thousands of hectares of forests (Mulvey & Lamb, 2012).

Insect outbreaks such as that caused by ALM are seldom distributed uniformly across a forested landscape. What determines the magnitude of impact of defoliators at a particular place and particular time is often difficult to determine (Zurell, Jeltsch, Dormann, & Schroder, 2009). Because they are poikilothermic, the population dynamics of insects depends on the environmental conditions of the landscape within which they live. Temperature and precipitation can play central roles in determining survival, spatial extent, and abundance of insect populations (Berryman, 1996).

Estimates of extent, distribution, and impacts of forest insect pests such as the ALM are mostly made based on aerial surveys. Since aerial survey coverage is limited in Alaska because of its size, much of the forest area infested by insect pests, unavoidably, goes uncounted. At most, only 25% of the approximately 51 million ha of forested area in the state is surveyed in any one year. During 2010, 183,588 ha in Alaska were noted as infested with ALM (Lamb & Winton, 2011), which is certainly an underestimate since area between flight lines was not assessed. Nonetheless, this statistic is used in statewide, regional, and national summaries for pest conditions. The need for accurate and timely assessments of pest conditions is increasingly important (Erdle & MacLean, 1999; Smith et al., 2005) as they are used by forest managers to compose forest health reports, develop risk maps, evaluate effectiveness of pest management efforts, develop research priorities, predict yields of various forest products, and make other decisions about future forest resource investments.

Assessments might be more accurate if the areas omitted during the survey flights could be taken into consideration. Cost effective methods for predicting pest conditions between flight lines could be very useful. Recent work to model the spatial distribution of insect pests and diseases using roadside surveys, field plots, satellite imagery, and spatial statistics offers some promise for providing more complete coverage of pest distributions. Reich, Lundquist, and Bravo (2004) and Lundquist and Reich (2006), for example, have presented methods of predicting the spatial distribution and severity of forest insect pests and diseases in the Black Hills of South Dakota using Landsat TM satellite imagery linked to field plots and a selection of auxiliary GIS data layers. Through this study, we expand on these methods to model forest insect pest distributions in Alaska.

Our long-range goal was to eventually develop methods to model the statewide spatial distributions of major insect pests in this state. Aspen leaf miner was used here as a case study because infested trees are unusually visible from the road, the air, and in satellite imagery. In this study, our objectives were to: (a) model the spatial distribution of ALM as a function of climatic conditions, and (b) estimate severity of the damage caused by the ALM as a function of climatic conditions. To assess the accuracy of these climate-based assessments, results were compared to independent estimates obtained using satellite imagery in combination with the data collected from a roadside survey.

MATERIAL AND METHODS

Roadside Survey

In the summer of 2010, a roadside survey was conducted along the major highways (Parks, Glenn, Dalton, Elliott, Seward, and Richardson Highways) in the interior and south central Alaska covering approximately 2,400 km from Seward (latitude 60° N) in the south to the southern slopes of the Brooks Range (latitude 68° N) in the north. A total of 318 sample points was geo-referenced using a global positioning system (Model GPS 76CSx, Garmin International, Inc., Olathe, KS, USA) with an accuracy of $\pm$ 3 m. Damage to aspen on both sides of the road at these sample points was visually estimated during late-July to early-August using assessment keys (Figure 1), located approximately every 8 km (5 mi) along the highways (Schomaker et al., 2007). Severity of damage was scored using a scale ranging from 0 (*healthy*) to 5 (*severely damaged*) (Figure 1).

Climate Zones

Geographic information system (GIS) raster layers representing the long-term (50 yr) average monthly temperatures (°C) and precipitation (mm) for the state were obtained from the United States Geological Survey (USGS) Alaska Science Center, High Altitude Climate Transects at a 1,000-m resolution. These layers were used to define five temperature zones and five precipitation zones in combinations that defined 25 unique climatic zones

FIGURE 1 Severity intensity diagram used to assess infested aspen trees showing scores from 0 = not infested (left), to 3 (middle), to 5 = heavily infested (right).

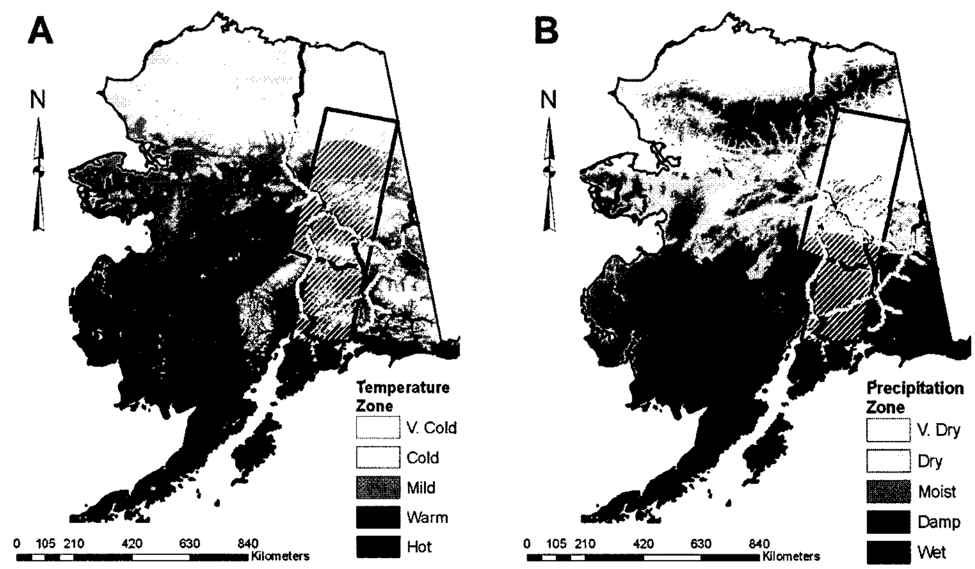

FIGURE 2 (A) Temperature and (B) precipitation zones in the state of Alaska. The cross-hatched rectangular region is the area covered by Landsat-5 TM imagery, while the white circles along the road network represent sample sites.

(Figure 2; Reich, Aguirre-Bravo, & Bravo, 2008). The climate zones were based on a histogram equalization approach that produced a uniform distribution of temperatures and precipitations across the state (Acharya & Ray, 2005). This produces a somewhat linear relationship between the average temperature and precipitation associated with a given climate zone and the classes used to denote the climate zones. Zonal statistics were used to summarize the variability in temperatures and precipitation in each of the 25 climate zones (Table 1).

TABLE 1 Summary Statistics of Average Temperatures and Precipitation in Alaska by Climate Zone

Climate zone	Min	Mean	Max	CV%
Precipitation (mm)				
1-Very dry	4.6	14.8	20.6	27.8
2-Dry	20.7	25.0	29.1	9.0
3-Moist	29.2	33.0	37.5	7.1
4-Damp	37.6	46.2	62.0	14.1
5-Wet	62.1	116.0	275.5	36.0
Temperature (°C)				
1-Very cold	−34.3	−12	−10.2	15.9
2-Cold	−10.1	−8.6	−7.4	9.3
3-Mild	−7.3	−6.2	−5.1	10.7
4-Warm	−5.0	−3.6	−2.1	23.4
5-Hot	−2.0	1.0	9.0	243.8

Presence of the Aspen Host

A 30-m raster layer of the major vegetation types was obtained from the Alaska Department of Natural Resources (http://dnr.alaska.gov/commis/pic/maps.htm). The raster layer of vegetation types was converted to a binary surface indicating the presence/absence of aspen in the state. The binary surface was resampled to 1,000-m resolution using a majority rule in the Spatial Analyst of ArcGIS (Version 9.3) to produce aggregated patterns similar to what might be available if the vegetation types were mapped at coarser spatial resolutions (Benson & MacKenzie, 1995). The resampling was done in increments. The 30-m raster layer was resampled to 100 m, then to 300, m and then finally to 1,000 m. The frequency of raster cells classified as aspen was determined for each of the 25 climate zones. Frequency as used in this article is defined as the number of 1000-m raster cells classified as aspen in a given climate zone.

Multiplying the frequencies by 100 provides an estimate of the area (ha) classified as aspen, $\mathcal{A}$ (A), in each climate zone. Following the classical interpretation of probabilities, the probability of observing aspen, $\mathcal{P}$ (A), was defined as the ratio of the number of raster cells classified as aspen, $\mathcal{A}$ (A), divided by the total number of raster cells in a climate zone. Probabilities were summarized in a 5 × 5 Climate Transition Matrix (CTM) representing the response in the probability of observing aspen to changes in climatic conditions (Table 2). The rows of the matrix correspond to the five temperature zones and the columns the five precipitation zones. This information was used to develop a raster layer of the probability of observing aspen throughout the state as a function of climatic conditions.

Presence and Severity of the Aspen Leaf Miner

Using the data from the 2010 roadside survey, the probability of observing ALM given the presence of the aspen host, $\mathcal{P}$ (M|A), was estimated for each climate zone as the proportion of aspen sites infested with ALM. Because of the subtle differences between severity codes and the potential

TABLE 2 Climate Transition Matrix (CTM) of the Conditional Probability of Observing Aspen Within the Temperature and Precipitation Zones in Alaska

	Precipitation zones				
Temperature zone	1	2	3	4	5
1	.0110	.0111	.0047	.0012	.0002
2	.0403	.0415	.0435	.0172	.0028
3	.1316	.0940	.0911	.0314	.0049
4	.1066	.0795	.0528	.0334	.0096
5		.0625	.0174	.0215	.0032

TABLE 3 Climate Transition Matrix (CTM) of the Conditional Probability of Observing Aspen Leaf Miner Given the Presence of the Aspen Host Within the Temperature and Precipitation Zones in Alaska

	Precipitation zones				
Temperature zone	1	2	3	4	5
1	**.01**	**.36**	**1.00** (.00)	**1.00**	**1.00**
2	**.04** (.00)	**.65** (1.00)	**1.00** (.00)	**1.00**	**1.00**
3	**.27** (1.00)	**1.00** (1.00)	**1.00** (1.00)	**1.00** (1.00)	**.71**
4	**1.00** (1.00)	**1.00** (.98)	**1.00** (.90)	**.31** (1.00)	**.03** (.50)
5		**1.00**	**.66** (.25)	**.05** (1.00)	**.00** (.00)

Note. The numbers in bold are predicted probabilities and the numbers in parentheses are the observed probabilities.

for misclassification, it was decided to place the infested aspen sites into one of two groups based on the severity of the damage: low severity (severity code 1 or 2) and high severity (severity code 3, 4, or 5). This information was used to estimate the probability of observing an infestation with a low or high severity given the presence of ALM, $\mathcal{P}$ (S|M). Probabilities were summarized in a 5 x 5 CTM. About a third of the CTMs contained missing values since not all climate zones were sampled in the roadside survey (Table 3).

Influence of Climate on Distribution of Aspen and ALM

Linear and polynomial regression analyses were applied to patterns in the probabilities of observing aspen, ALM, and severity of the infestation on the CTMs as a function of the temperature (T = 1, 2, 3, 4, 5) and precipitation (P = 1, 2, 3, 4, 5) zones. The form of the regression model was chosen based on the assumption that a species response to environmental factors generally follow either a linear (Reich, Bonham, Aguirre-Bravo, & Chazaro-Basañeza, 2010) or curvilinear relationship (Grime, 1979). Based on preliminary analysis, a natural logarithm transformation was used to stabilize the variability in the probabilities across climate zones, while the integers (1, 2, 3, 4, 5) were used to identify the temperature and precipitation zones in the model. The linear relationship between climate zones and temperature and precipitation is a property of the histogram equalization technique used in defining the zones (Table 1). To account for the spatial structure in the probability data among the CMTs, a spatial error model was used to estimate the parameters of the model (Upton & Fingleton, 1985):

$$\begin{aligned} y &= X\beta + \varepsilon, \\ \varepsilon &= \lambda W\varepsilon + \eta, \end{aligned} \tag{1}$$

where y is the dependent variable, X is a design matrix of independent variables, β the regression coefficients, W is a binary spatial weights matrix used to define the joins of the 5 × 5 CTM following the chess move for a rook (up, down, left, right), $-1 < \lambda > 1$ is a measure of the degree of spatial correlation, ε are spatially correlated errors, and $\eta \sim N(0, \sigma^2)$ spatially independent errors. A step AIC was used to select the subset of climate variables (temperature and precipitation zones) to include in the models (Venables & Ripley, 2002). A likelihood ratio test was used to test the null hypothesis that the spatial models were better than ordinary least squares, which assumes that the errors are spatially independent (H_o: $\lambda = 0$). Moran's I was used to test the residuals for spatial autocorrelations. The *p*-values associated with the Moran's I test statistic were calculated under the randomization assumption (Upton & Fingleton, 1985). All analyses were done with the R statistical package (R Development Core Team, 2008).

The fitted models were used to estimate missing probabilities in the CTMs for the probability of observing ALM given the aspen host, $\mathcal{P}$ (M|A), and the probability of the severity of the infestation given the presence of ALM, $\mathcal{P}$ (S|M). Probabilities were truncated ensuring no forecasts were greater than unity. The completed CTMs were used to develop raster layers of the probabilities of observing ALM and the severity of the ALM infestation throughout the state. The final surfaces developed from the fitted models are particularly reliant on the assumption that the structural form of the regression models accurately describes the relationship between temperature and precipitation and the probability of observing ALM and severity of the infestation even in the climate zones not sampled in the roadside survey. It is recognized that the further the models extrapolate outside the range of observed climate zones, the more chance there is that the models will fail due to differences between the assumptions and the sample data and the true values. While there is no way to test the validity of the final models without additional field sampling, one can assess the error in estimation by placing prediction intervals around the estimated probabilities.

Area Estimates

Multiplying the probability of observing aspen in a given climate zone by the probability of observing ALM given the aspen host provides an estimate of the probability of observing ALM in each climate zone: $\mathcal{P}(M) = \mathcal{P}(A) * \mathcal{P}(M|A)$. Multiplying these probabilities by the area of each climate zones provides an estimate of the area of infested aspen in each climate zone: $\mathcal{A}(M) = \mathcal{P}(M) * \mathcal{A}(C)$. Summing across all climate zones provides a statewide estimate of the extent of the ALM infestation. To estimate the extent of infestations with a low severity (S_L), the area estimates of ALM were multiplied by the probability of an infestation with a low severity:

$\mathcal{A}(S_L) = \mathcal{P}(S_L|M) * \mathcal{A}(M)$. The extent of the infestations with a high severity (S_H) was obtained by subtraction: $\mathcal{A}(S_H) = \mathcal{A}(M) - \mathcal{A}(S_L)$.

Model Validation

To validate the use of climate zones in predicting the extent and severity of ALM in Alaska, a smaller region covering approximately 20.2 million ha (13% of the state) from the Kenai Peninsula in the south, to north of Fairbanks was selected (Figure 2). Thirty-one Landsat-5 TM images were obtained from the Earth Resources Observation and Science (EROS) Data Center (Sioux Falls, South Dakota) to cover this region. The date of imagery acquisition corresponded to the 2010 roadside survey. The Landsat-5 TM imagery had six spectral bands with a 30-m resolution and one band with a 60-m resolution. This latter band was re-sampled to a 30-m spatial resolution using nearest neighbor techniques (Muukkonena & Heiskanenb, 2005). Nearest neighbor re-sampling was selected to provide faster computer processing than other interpolation methods. In addition, nearest neighbor interpolation better maintains original reflectance values, provides sufficient accuracy, and reduces potential introduction of unwanted geometric distortions in areas with no ground control points to provide precise control (Muukkonena & Heiskanenb, 2005).

Topographic data were taken from a digital elevation model (DEM) obtained from the National Elevation Dataset (NED) as a seamless raster (ArcGIS Desktop, Version 9.3) at a 90-m resolution (USGS; Gesch et al., 2002; Rabus, Eineder, Roth, & Bamler, 2003). The DEM was re-sampled to a 30-m spatial resolution using bilinear techniques (Edenius, Vencatasawmy, Sandstrom, & Dahlberg, 2003), producing a more continuous surface reflecting gradual changes in elevation at a 30-m spatial resolution. GIS grids of elevation, slope, and aspect were derived from the DEM using ArcGIS (Version 9.3). Values for all grid layers of information were derived for each sample location in the 2009 roadside survey using ArcGIS.

Binary classification trees (Brieman, Friedman, Olshen, & Stone, 1984) were used to predict the presence/absence and severity of the aspen leaf miner (ALM) infestation within this region using data from the 2010 roadside survey. Independent variables considered in the trees were topography (elevation, slope, aspect) and various bands of satellite imagery. A 10-fold cross-validation procedure was used to identify the best tree size to minimize the prediction classification error. The pruned classification trees were used to develop GIS layers displaying the spatial distribution of the presence/absence and severity of the ALM infestation at a 30-m resolution. This was accomplished by passing the appropriate GIS layers of topographic data and spectral bands from the satellite imagery through the pruned classification trees.

The predictive accuracy of the binary models was measured using the area under the receiver operating curve (ROC; Boyce, Vernier, Nielsen, & Schmiegelow, 2002). The area under the curve (AUC) is a measure of discrimination, or the ability of the model to correctly classify a sample point (Boyce et al., 2002). An area of 1 represents perfect prediction, while an area of 0.5 represents a prediction equivalent to random chance. A rough guide for classifying the accuracy of a model is the traditional academic point system: (0.90 to 1.0 = excellent; 0.80 to 0.89 = good; 0.70 to 0.79 = fair; 0.60 to 0.69 = poor; less than 0.60 = fail). By varying the size or the number of terminal nodes in a tree, a series of classification trees are generated, each with a different sensitivity and specificity. The set of sensitivity-specificity combinations define a curve that can be used like an ROC curve. Every point on the ROC curve corresponds to a binary classifier, for which one can calculate the classification accuracy and other measures of fit such as point estimates of the AUC. All analyses were done with the R statistical package (R Development Core Team, 2008).

Estimates of the extent and severity of the ALM in the region covered by the satellite imagery was determined by counting the number of 30-m raster cells classified as being infested with ALM and by severity classes. Counts were multiplied by 0.09 to obtain estimates in hectares. This information was compared to estimates obtained from the statewide model. Area estimates were obtained by weighting the probability of observing ALM given the aspen host or severity of the infestation proportional to the distribution of climate zones in the region.

RESULTS

Spatial Distribution of Aspen

Aspen was a dominant vegetation type in 24 of the 25 climate zones covering an area of more than 5.7 million ha or about 4% of the total land area in the state (Figure 3a). A second-degree polynomial was used to describe the relationship between the temperature and precipitation zones and the probability of observing aspen (Table 4). The spatial autoregressive model accounted for 96% of the variability observed in the probabilities of observing aspen in a given climate zone (Table 4). The frequency of observing aspen as the dominant vegetation type was highest throughout the central region of the state (Figure 3a). The climate of this region has low to moderate levels of precipitation (P = 1, 2, and 3) and cold to mild temperatures (T = 2, 3, and 4; Table 1, Figure 2). The highest probability of observing aspen was in the mild-very dry (T = 3, P = 1) region of the state. Aspen also occurred in the hottest and wettest regions of the state. This area corresponds to a population of aspen found on the Kenai Peninsula and might be regarded as a separate population and thus be treated in a distinctive fashion. Except for

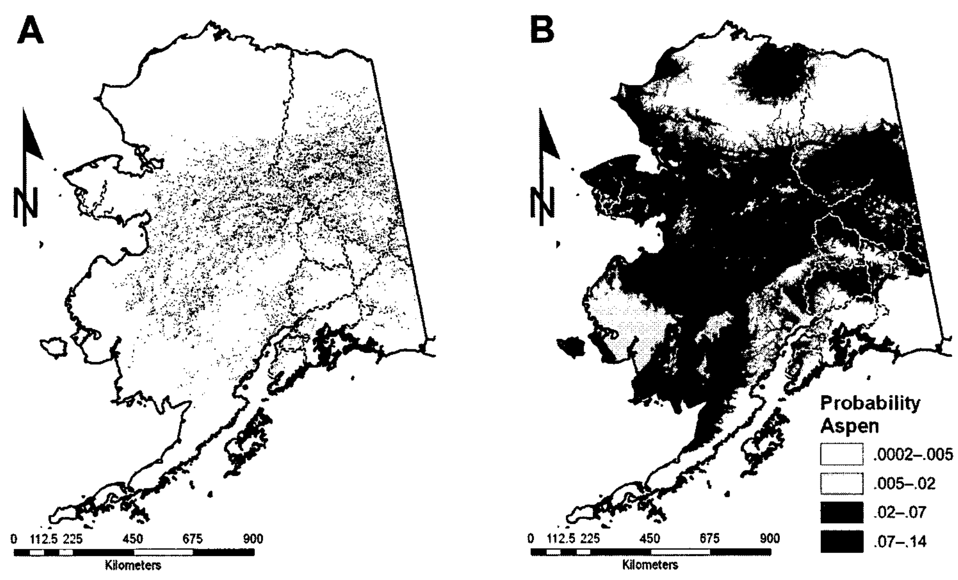

FIGURE 3 (A) Spatial distribution of dominant aspen stands; and (B) the probability of observing aspen, $\mathcal{P}$ (A), in the state of Alaska.

this one case, the probability of observing aspen generally decreased with increasing precipitation. The probability of observing aspen was lowest in the very coldest (T = 1) and hottest (T = 5) regions of the state, irrespective of precipitation (Figures 2 and 3).

Spatial Distribution of Aspen Leaf Miner

A second-degree polynomial was used to model the relationship between the temperature and precipitation zones and the probability of observing ALM given the presence of the aspen host (Table 4). The spatial autoregressive model accounted for 83% of the variability observed in the probabilities of observing ALM given the presence of aspen (Table 4). Aspen leaf miner was observed or estimated to occur on almost 100% of the aspen sites in 13 of the 24 climate zones (Table 3). These 13 climate zones define a temperature-precipitation gradient that forms the diagonal of the CTM. It starts in the lower left corner of the CTM which represents a hot-very dry climate (T = 5, P = 1) and stretches to the upper right corner of the CTM representing a very cold-wet climate (T = 1, P = 5). These 13 climate zones characterize the central region of the state (Figure 4a). In the very cold-very dry climate zones (T = 1, 2, P = 1, 2) and the hot-wet climate zones (T = 4, 5, P = 4, 5), the ALM was either not detected on the sample plots or it occurred at very low frequencies. These climate zones represent the northern most and southern most regions of the state as well as the eastern part of the central region of the state (Figure 4a).

TABLE 4 Spatial Autoregressive Models Describing the Spatial Variability in the Probability of Observing Aspen, ALM, and the Severity of the ALM Infestation as a Function of the Temperature and Precipitation Zones in Alaska

Parameter[¶]	Probability aspen $\mathcal{P}$ (A)	Probability ALM given aspen $\mathcal{P}$ (M|A)	Probability low severity given ALM $\mathcal{P}$ (S_L|M)
Intercept	−7.528 (0.342)	−12.750 (3.957)	13.688 (7.295)
Temp zone (T)	2.967 (0.168)	3.031 (1.186)	−4.196 (2.055)
Precip zone (P)	.607 (0.171)	6.404 (1.389)	−6.495 (2.594)
T^2	−.477 (0.027)		
P^2	−.273 (0.027)	−.417 (0.198)	
TP	.115 (0.024)	−1.219 (0.388)	1.762 (0.203)
λ	−.474 (0.204)	−.747 (0.148)	−.620 (0.203)
R^2	.998	.875	.646
FIT[‡]	.971	.830	.473
AICc	23.6	65.7	64.9
Likelihood ratio[†]	2.851 (0.091)	6.159 (0.0.013)	2.981 (0.084)
Moran's I on residuals[*]	−.090 (0.769)	−.189 (0.626)	−.177 (0.609)
Sample size	24	13	12

Note. The numbers in parentheses are the estimated standard errors.

[¶]Model: $Y = X\beta + \varepsilon$, where $\varepsilon = \lambda W\varepsilon + U$; Y = dependent variable; X = matrix of independent variables; W = spatial weights matrix; $-1 < \lambda < 1$, measures of spatial correlation; ε = spatially correlated errors from the regression model, $U \sim N(0,1)$ spatially independent errors. The spatial weights matrix is based on the rook's move.

[‡]The correlation between the observed and predicted values squared. This may be a more reliable estimate of model fit than R^2 for the spatial models.

[†]Test the null hypothesis of no spatial autocorrelations in the residuals of the regression model (H_0: $\lambda = 0$). The *p*-value associated with the test statistic is given in parentheses.

[*]Test the null hypothesis the residuals of the regression model are spatially independent after adjusting for the presence of spatial autocorrelation in the data. The *p*-value associated with the test statistic is given in parentheses.

The probability of observing ALM in a given climate zone followed a pattern similar to aspen (Figure 4b). Differences were in the colder and drier climate zones where the probability of detecting ALM decreased to near zero. For example, probability of observing ALM in the mild-very dry climate zone ($T = 3$, $P = 1$) was near zero, even though the probability of observing aspen was highest in this climate zone. Differences in climatic conditions optimal for the presence of either aspen or ALM (i.e., lack of spatial synchronization) may limit the overall impact the insect is having on the aspen populations. Based on reports in annual Forest Conditions Reports beginning in 2000 and distributed by the USDA Region 10 Forest Health Protection, the estimated distribution of ALM corresponds closely to known "hot spots" for ALM (the area near Glennallen in the south, along the Alaska Highway between Delta Junction and Tok, the Fairbanks area, Yukon Flats, Yukon River Valley, and the Tanana River Valley; Lamb & Winton, 2011). Little is know about the west-central part of the state because of limited access by road and so it was not possible to validate the model for this area. This would entail establishing a study site similar to the one used in this study in the western part of the

TABLE 5 Estimates of the Extent of Aspen, the Area of Aspen Infested With the Aspen Leaf Miner, and the Area With Low and High Levels of Infestation by Climate Zones in the State of Alaska

Climate zone	Area of climate zones (ha) A (C)	Area of aspen (ha) A (A)	Area of ALM (ha) A (M)	Area of low severity (ha) A (S_L)	Area of high severity (ha) A (S_H)
11, V. cold-V. dry	7,736,000	85,400	606	606	0
12, V. cold-Dry	5,129,800	56,700	20,531	20,531	0
13, V. cold-Moist	4,884,300	22,800	22,800	205	22,595
14, V. cold-Damp	5,667,600	6,800	6,800	1	6,799
15, V. cold-Wet	2,165,600	400	400	0	400
21, Cold-V. dry	9,092,100	366,300	15,751	15,751	0
22, Cold-Dry	5,634,500	234,000	153,293	80,142	73,152
23, Cold-Moist	2,724,000	118,600	118,600	3,178	115,422
24, Cold-Warm	2,292,500	39,400	39,400	55	39,345
25, Cold-Hot	2,782,100	7,800	7,800	1	7,799
31, Cool-V. dry	6,884,500	905,900	240,245	214,971	25,274
32, Cool-Dry	9,761,600	917,400	917,400	244,762	672,638
33, Cool-Moist	6,506,300	592,500	592,500	47,104	545,396
34, Cool-Damp	4,318,200	135,800	135,800	3,218	132,582
35, Cool-Wet	2,849,100	13,900	9,898	70	9,828
41, Warm-V. dry	898,800	95,800	95,800	7,511	88,289
42, Warm-Dry	8,688,100	690,900	690,900	94,031	596,869
43, Warm-Moist	11,964,000	631,600	631,600	149,247	482,353
44, Warm-Damp	8,411,400	281,000	86,267	35,387	50,880
45, Warm-Wet	3,720,300	35,700	1,189	847	342
52, Hot-Dry	6,400	400	400	28	372
53, Hot-Moist	7,382,600	128,700	84,697	59,458	25,240
54, Hot-Damp	11,701,100	251,900	12,217	12,217	0
55, Hot-Wet	16,509,600	52,100	83	83	0
Total area (ha)	147,710,500	5,671,800	3,884,978	989,405	2,895,574
Percent				25.5	74.5
Percent of aspen			68.5	17.4	51.1

state. Assuming the underlying assumptions of the models are correct, it is estimated that 3.9 million ha or 68% of the aspen are infested with ALM (Table 5).

Severity of the ALM Infestation

A second-degree polynomial was used to model the relationship between the temperature and precipitation zones and the probability of observing an infestation of low severity (Table 4). The spatial autoregressive model accounted for 47% of the variability observed in the probabilities of observing low severity infestations (Table 4). The low FIT statistic suggests that there are factors other than temperature and precipitation that influence the severity of the infestation. The spatial distribution of aspen stands with low severity infestations occurred primarily in the northern portion of the range

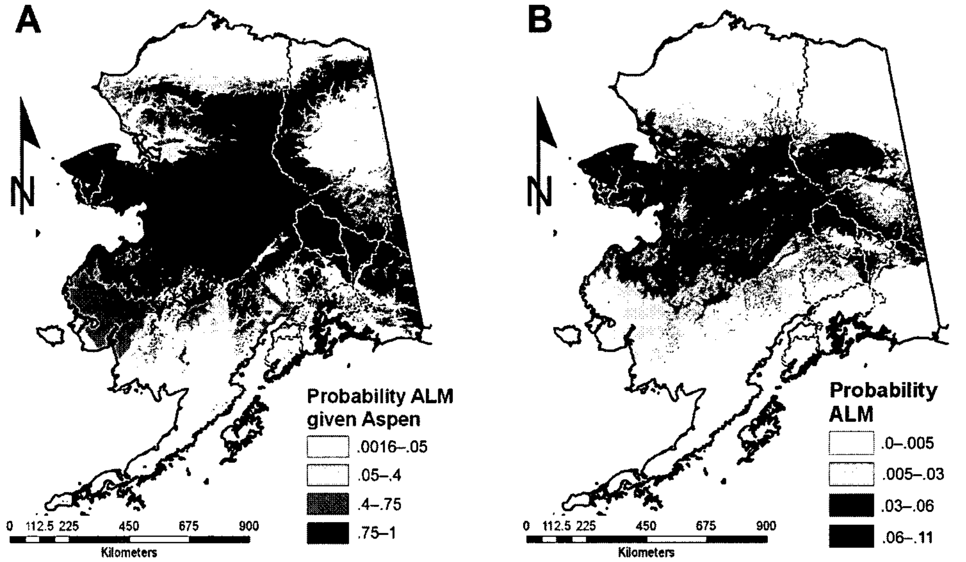

FIGURE 4 (A) Probability of observing aspen leaf miner (ALM) given the presence of the aspen host, $\mathcal{P}$ (M|A), and (B) the probability of observing ALM, $\mathcal{P}$ (M), in the state of Alaska.

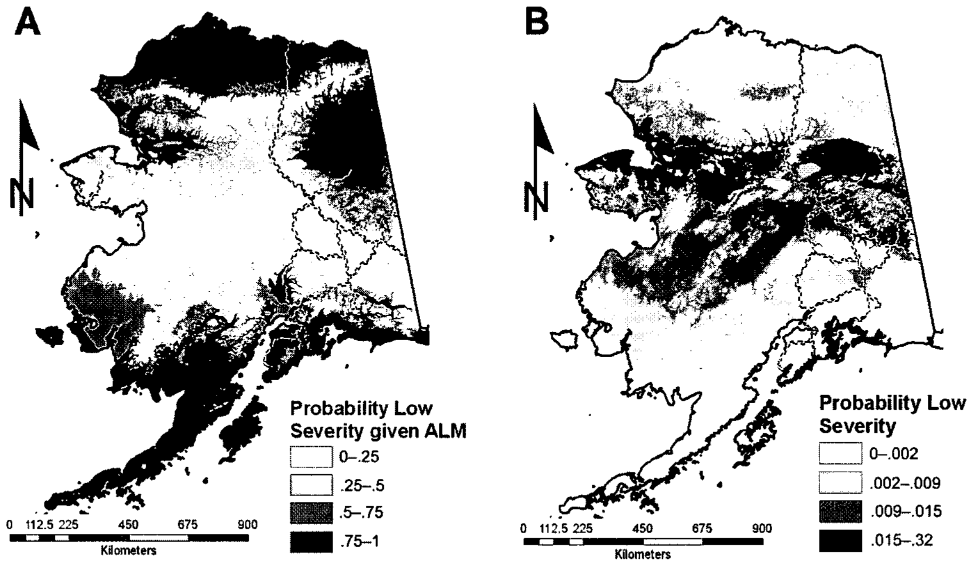

FIGURE 5 (A) Probability of observing a low severity infestation given the presence of the ALM, $\mathcal{P}$ (S_L |M); and (B) the probability of observing low severity infestation, $\mathcal{P}$ (S_L), in the state of Alaska.

of ALM (Figure 5), while infestations of high severity were located in the southern extent of the range of ALM (Figure 6).

It is estimated that there are 1 million ha of infested aspen with low severity and 2.9 million ha with high severity (Table 5). The infested aspen

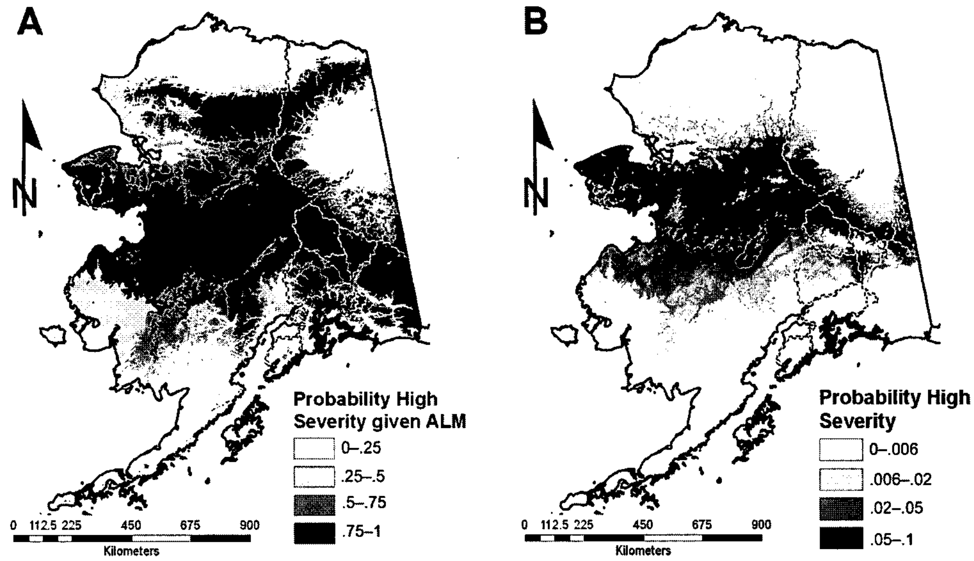

FIGURE 6 (A) Probability of observing a high severity infestation given the presence of the ALM, P (S_H |M); and (B) the probability of observing high severity infestation, P (S_H), in the state of Alaska.

sites classified as having low severity had an average severity code of 1.5, split evenly among the two severity classes (1 and 2). Sample observations classified as high severity had an average severity code of 3.4 on a scale from 3 to 5, and with approximately two-thirds of the aspen sites having a severity code of 3.

Predicting ALM and Severity Using Satellite Imagery and Topography

The final pruned classification tree for predicting the presence or absence of ALM in the study region covered by Landsat imagery had overall accuracy of .73, where accuracy is defined as the proportion of sample plots correctly classified. The area under the curve (AUC) was .74, indicating the model was average at discriminating between the presence and absence of ALM (Table 6). Variables important in predicting the presence of ALM included three Landsat bands (4, 6, and 7) and elevation. The three satellite bands were the most important variables used in the classification tree to distinguish between the distinct grayish-silver tone of infested trees and the non-infested trees. When implemented in GIS, the model indicated that ALM occurred unevenly across the study area, with the northern region of the study area showing a high frequency of occurrence. These areas represent the potential occurrence of ALM based on the spectral reflectance of the vegetation and topography.

The final pruned classification tree for the severity of the infestation had an overall accuracy of .73. Variables important in discriminating among

TABLE 6 Comparison of the State-Wide Model and Binary Classification Trees Using Landsat-5 TM imagery in Predicting the Extent and Severity of Aspen Leaf Miner in a 20 Million-ha Study Area in the Central Interior of Alaska

	State-wide model		Classification tree				
Class	Area (ha)	Percent	Area (ha)	Percent	ACC[4]	AUC[5]	Model ranking[6]
Low severity class (1–2)	212,930	31.0[1]	62,809	8.0[1]	.37	.68	Poor
High severity class (3–5)	474,891	69.0[1]	720,409	92.0[1]	.98	.67	Poor
Aspen leaf miner	687,820	37.4[2]	783,218	42.6[2]	.84	.74	Average
Aspen	1,838,465	9.1[3]	1,838,465	9.1[3]			
Total area	20,202,200		20,202,200				

[1]Percent of infested aspen in a severity class.
[2]Percent of aspen infested with ALM.
[3]Percent of study area classified as aspen at 30-m spatial resolution.
[4]Proportion of sample observations correctly classified.
[5]Area under the curve used to measure the predictive performance of the binary classification tree.
[6]Ranking of the predictive performance of the binary classification tree based on the AUC.

severity classes included two Landsat bands (3 and 5) and elevation. Landsat band 3 was the most important variable in distinguishing between severity classes. High spectral reflectance indicated severely infested aspen stands. The performance of the model as measured by the AUC was poor for both severity classes (Table 6). The classification tree only classified 37% of the low severity sample sites correctly compared to 98% for the high severity class. The misclassification of low severity sample sites as high severity lowered the overall performance of the model in accurately predicting aspen stands with high severity.

Comparison of the Two Approaches

The region used to compare the two approaches for estimating the extent and severity of the ALM infestation in the state covered 20.2 million ha (Figure 2). Aspen covered 1.8 million ha, or 9% of this region (Table 5). Applying the statewide model to this smaller region using the area associated with each of the climate zones that occurred within the region provided an estimate of 687,820 ha, or 37%, of the stands dominated by aspen were infested with ALM. This compares favorably with the classification tree that estimated 783,218 ha, or 43% of the aspen were infested with ALM, a difference of only 6%. This discrepancy may be due to differences in the spatial resolution used in developing the models. The probability of observing aspen at the state level was based on a 1,000-m spatial resolution, and many small aspen stands may have been excluded from the analysis. This would result in an underestimation of the area of aspen and subsequently the area infested with ALM.

The largest difference observed between the two models was in estimating the area associated with the severity of the infestation. The statewide model estimated that 69% of the aspen had a high severity infestation and 31% had low severity infestation (Table 6). In contrast, the classification tree estimated that 92% of the infested aspen had a high severity and only 8% with low severity. Considering that about one-third of the high severity classes should have been classified as low severity (i.e., classification errors), this would suggest that approximately 60% of the aspen sites should have been classified as having high severity and 40% low severity. This is more in agreement with the statewide model. This also underscores the expected difficulty of using satellite imagery to identify low level infestations or infestations that are not uniquely distinguishable on the satellite imagery.

DISCUSSION

Because of its size, Alaska presents a unique challenge for pest surveys. One objective of this study was to explore how existing aerial survey methods and results compare with recently developed spatial modeling techniques. In this regard, the Forest Conditions Report for 2010 noted ALM on 183,588 ha (Lamb & Winton, 2011). Since this estimate includes only those areas actually visually observed by the aerial surveyors within the flight path and the flight path covers at most 25% of the forested area, it is undoubtedly lower than the actual area infested. The spatial models estimate that the actual infested area was 3,884,978 ha in 2010, which is more than 21 times more extensive than that reported during the annual survey. By not including areas between the flight lines, most of the infested forest in Alaska goes unaccounted. The difference is considerable.

Distribution models like those developed here greatly add to assessments of the relative importance of various types of disturbances and in doing so, offer arguments for which disturbances should or should not be managed, and which disturbances might significantly impact forest health. With these maps, the spatial distribution, extent, and abundance of different disturbances can be estimated, and spatial prescriptions developed. They offer a useful guide to resource managers, and for choosing among available options. They help decision makers identify the locations of especially heavy damage caused by insects and other disturbances, estimate and predict where resource values are changed by insect pests and the impact of these changes on ecosystem services, and prioritize and decide on the best kinds of management options and where to implement them (Conard, Hartzell, Hilbruner, & Zimmerman, 2001). The value of these maps, however, is dependent on their accuracy.

Comparison of the climate-based spatial models with that developed using satellite imagery suggests pros and cons of these two approaches.

First, the climate-based models are not able to identify which particular aspen stands are infested, unlike the models based on satellite imagery. Nonetheless, both approaches produced similar estimates of the total infested acreage. Second, the climate-based models were able to estimate area associated with both low and high severity of infestation, unlike the model based on satellite imagery which classified most of the infestation as being high. Whether these differences reflect differences in accuracy of the data derived from roadside assessments and satellite imagery, or inappropriate prediction algorithms is difficult to determine. More likely, these differences are caused by a combination of all these causes. Assessment errors associated with aerial surveys as currently conducted are not known. However, the spatial models developed in this study offer a means to calculate both accuracy and error.

The use of climatic zones, as defined here, provides a useful perspective on the effects of temperature and precipitation on insect dynamics and distribution and provides opportunities for quantifying relationships between forest insect populations and environmental factors (Guisan & Zimmermann, 2000). Insect populations respond to conditions within climatic zones in many ways—including altered assemblage composition, range extension and contraction, changes in ecological roles and interactions and the impacts of these interactions, and changing phenological timing of life history events (Burnett, 1949; Danks, 1992; Ayres, 1993; Hiliövaara & Peltonen, 1999; Bale et al., 2002; Logan, Regniere, & Powell, 2003; Dukes et al., 2009). Such relationships can be used as a basis to predict abundance of forest insects in zones with similar climatic conditions or to predict how insect populations will change under different scenarios of changing temperature and/or precipitation.

Strong, but mostly circumstantial, evidence exists for climate-driven changes in the behavior and distribution of a handful of insects in the state of Alaska and elsewhere (Wolken et al., 2011). For example, large populations of large aspen tortrix (*Choristoneura conflictana*) and the spear-marked black moth—*Rheumaptera hastate* (L.); Lepidoptera: Geometridae—previous to 1980 have given way to much lower populations thereafter (Werner, 2007). Furthermore, previously low populations of spruce budworm (*Choristoneura fumiferana* Freeman), spruce cone moth (*Cydia strobilella*), larch sawfly (*Pristiphora erichsonil*; Hymenoptera: Tenthredinidae) and aspen leaf miner have all increased dramatically after 1990 (Werner, 2007). Juday (1998) described the populations of spruce beetle in south-central Alaska during the 1990s as "the largest ever documented from an insect outbreak in North America," and claimed that climate was the driving factor. In fact, Berg, Henry, Fastie, De Volder, and Matsuoka (2006) linked the 1990s spruce beetle outbreak to a series of years (1987–1997) with higher than average summer temperatures. Such effects will probably become more apparent in time.

An appropriate long-range goal for forest entomologists is to develop methods to model how climate change will affect spatial distributions of major insect pests. Temperature-driven models of the impacts of climate change on insect abundance have been developed for a number of insects. Mechanistic models based on temperature impacts on voltinism and applicable to Alaska have been developed for spruce beetle (Hansen, Bentz, & Turner, 2001a, 2001b). Our limited understanding the influence of large-scale temperature and precipitation patterns on insect pests restricts our ability to predict future impacts of these agents on forest health. Our results suggest that the climate transition matrices would be useful for examining the influence of temperature or precipitation on insect abundance and for predicting what might happen to insect populations under various environmental change scenarios.

Aspen leaf miner injury is unusually showy. Infested trees can be easily seen even from airplanes, satellites, and roadways. Similar work with insects that cause less obvious injuries is more immediately challenging because their effects might not be easily seen. Light infestations are much more difficult to discern than heavy infestations, even for ALM. As a consequence, the magnitude of an outbreak would be underestimated, and estimates of its distribution are much reduced. Holsten et al. (2009) list over 60 other Alaskan insect pests of which 12 were active enough to be assessed during the 2010 aerial survey of the Alaska Region Forest Health Protection unit. Each of these would no doubt present their own unique characteristics in assessment, but if they are visible enough to see from the air, they would probably be able to be modeled in a manner similar to the aspen leaf miner. In this regard, the aspen leaf miner is probably representative of the broader set of insect pests. Many of the hurdles faced with the aspen leaf miner would probably be faced with these other pests.

REFERENCES

Acharya, T., & Ray, A. K. (2005). *Image processing: Principles and applications*. Stafford, Australia: Wiley Interscience.

ArcGIS Desktop (Version 9.3) [Computer software]. Redlands, CA: Environmental Systems Research Institute.

Ayres, M. P. (1993). Plant defense herbivory and climate change. In P. M. Kareiva, J. G. Kingsolver, & R. B. Huey (Eds.), *Biotic interactions and global change* (pp. 75–94). Sunderland, MA: Sinauer Associates.

Bale, J. S., Masters, G. J., Hodkinson, I. D., Awmack, C., Bezemer, T. M., Brown, V. K., . . . Whittaker, J. B. (2002). Herbivory in global climate change research: Direct effects of rising temperature on insect herbivores. *Global Change Biology*, *8*, 1–16.

Benson, B. J., & MacKenzie, M. D. (1995). Effects of sensor spatial resolution on landscape structure parameters. *Landscape Ecology*, *10*, 113–120.

Berg, E. E., Henry, J. D., Fastie, C. L., De Volder, A. D., & Matsuoka, S. M. (2006). Spruce beetle outbreaks on the Kenai Peninsula, Alaska, and Kluane National Park and Reserve, Yukon Territory: Relationship to summer temperatures and regional differences in disturbance regimes. *Forest Ecology and Management*, *227*, 219–232.

Berryman, A. A. (1996). What causes population cycles of forest Lepidoptera? *Trends in Ecology & Evolution*, *11*, 28–32.

Boyce, M. S., Vernier, P. R., Nielsen, S. E., & Schmiegelow, F. K. A. (2002). Evaluation resource selection functions. *Ecological Modeling*, *157*, 281–300.

Brieman, L., Friedman, J., Olshen, R., & Stone, C. (1984). *Classification and regression trees*. Pacific Grove, CA: Wadsworth and Brooks.

Burnett, T. (1949). The effect of temperature on insect host-parasite population. *Ecology*, *30*, 113–134.

Conard, S. G., Hartzell, T., Hilbruner, M. W., & Zimmerman, G. T. (2001). Changing fuel management strategies—The challenge of meeting new information and analysis needs. *International Journal of Wildland Fire*, *10*, 267–275.

Condrashoff, S. F. (1964). Bionomics of the aspen leaf miner, *Phyllocnistis populiella* Cham. (Lepidoptera: Gracillariidae). *Canadian Entomologist*, *96*, 857–974.

Danks, H. V. (1992). Arctic insects as indicators of environmental change. *Arctic*, *45*, 159–166.

Dukes, J. S., Pontius, J., Orwig, D., Garnas, J. R., Rodgers, V. L., Brazee, N., . . . Ayres, M. (2009). Responses of insect pests, pathogens, and invasive plant species to climate change in the forest of northeastern North America: What can we predict? *Canadian Journal of Forest Research*, *39*, 231–248.

Edenius, L., Vencatasawmy, C. P., Sandstrom, P., & Dahlberg, U. (2003). Combining satellite imagery and ancillary data to map snowbed vegetation important to reindeer *Rangifer tarandus*. *Arctic, Antarctic and Alpine Research*, *35*, 150–157.

Erdle, T. A., & MacLean, D. A. (1999). Stand growth model calibration for use in forest pest impact assessment. *The Forest Chronicle*, *75*, 141–152.

Gesch, D., Oimoen, M., Greenlee, S., Nelson, C., Steuck, M., & Tyler, D. (2002). The national elevation dataset. *Photogrammetric Engineering & Remote Sensing*, *68*, 5–32.

Grime, J. P. (1979). *Plant strategies and vegetation process*. Chichester, UK: John Wiley.

Guisan, A., & Zimmermann, N. E. (2000). Predictive habitat distribution models in ecology. *Ecological Modeling*, *135*, 147–186.

Hansen, E. M., Bentz, B. J., & Turner, D. L. (2001a). Physiological basis for flexible voltinism in the spruce beetle (*Coleoptera: Scolytidae*). *The Canadian Entomologist*, *133*, 805–817.

Hansen, E. M., Bentz, B. J., & Turner, D. L. (2001b). Temperature-based model for predicting univoltine brood proportions in spruce beetle (*Coleoptera: Scolytidae*). *The Canadian Entomologist*, *133*, 827–841.

Hiliövaara, K., & Peltonen, M. (1999). Bark beetles in a changing environment. *Ecological Bulletins*, *47*, 48–53.

Holsten, E., Hennon, P., Trummer, L., Kruse, J., Schultz, M., & Lundquist, J. (2009). *Insects and Diseases of Alaskan Forests* (FHP Publication R10-TP-140). Anchorage, AK: USDA Forest Service, Alaska Region.

Juday, G. P. (1998). *Spruce beetles, budworms, and climate warming*. Retrieved from http://www.cgc.uaf.edu/Newsletter/gg6_1/beetles.html

Lamb, M., & Winton, L. (Eds.). (2011). *Forest health conditions in Alaska 2010* (FHP Protection Report R10-PR-23). Anchorage, AK: USDA Forest Service, Alaska Region.

Logan, J. A., Regniere, J., & Powell, J. A. (2003). Assessing the impacts of global warming on forest pest dynamics. *Frontiers in Ecology and the Environment, 1*, 130–137.

Lundquist, J. E., & Reich, R. M. (2006). Tree diseases, canopy structure, and bird distributions in ponderosa pine forests. *Journal of Sustainable Forestry, 23*, 17–45.

Mulvey, R., & Lamb, M. (Eds). (2012). *Forest health conditions in Alaska 2011* (FHP Protection Report R10-PR-25). Anchorage, AK: USDA Forest Service, Alaska Region.

Muukkonena, P., & Heiskanenb, J. (2005). Estimating biomass for boreal forests using ASTER satellite data combined with standwise inventory data. *Remote Sensing of Environment, 99*, 434–447.

R Development Core Team. (2008). *R: A language and environment for statistical computing*. Vienna, Austria: R Foundation for Statistical Computing. Retrieved from http://www.R-project.org

Rabus, B., Eineder, M., Roth, A. & Bamler, R. (2003). The shuttle radar topography mission—A new class of digital elevation models acquired by spaceborne radar. *Journal of Photogrammetry & Remote Sensing, 57*, 241–262.

Reich, R. M., Aguirre-Bravo, C., & Bravo, V. A. (2008). New approach for modeling climatic data with applications in modeling tree species distributions in the states of Jalisco and Colima, Mexico. *Journal of Arid Environments, 72*, 1343–1357.

Reich, R. M., Bonham, C. D., Aguirre-Bravo, C., & Chazaro-Basañeza, M. (2010). Patterns of tree species richness in Jalisco, Mexico: Relation to topography, climate and forest structure. *Plant Ecology, 210*, 67–84.

Reich, R. M., Lundquist, J. E., & Bravo, V. A. (2004). Spatial models for estimating fuel loads in the Black Hills, South Dakota, USA. *Internationl Journal of Wildland Fire, 13*, 119–129.

Schomaker, M. E., Zarnoch, S. J., Bechtold, W. A., Latelle, D. J., Burkman, W. G., & Cox, S. M. (2007). *Crown-condition classification: A guide to data collection and analysis* (General Technical Report SRS-102). Asheville, NC: USDA Forest Services.

Smith, A. H., Pinkard, E. A., Stone, C., Battaglia, M., & Mohammed, C. L. (2005). Precision and accuracy of pest and pathogen damage assessment in young eucalypt plantations. *Environmental Monitoring and Assessment, 111*, 243–256.

Upton, G., & Fingleton, B. (1985). *Spatial data analysis by example: Vol. 1—Point pattern and quantitative data*. New York, NY: John Wiley and Sons.

Venables, W. N., & Ripley, B. D. (2002). *Modern applied statistics with S* (4th ed.). New York, NY: Springer.

Wagner, D., DeFoliart, L., Doak, P., & Schneiderheinze, J. (2008). Impact of epidermal leaf mining by the aspen leaf miner (*Phyllocnistis populiella*) on the growth, physiology, and leaf longevity of quaking aspen. *Oecologic, 157*, 259–267.

Werner, R. A. (2007). Climate warming in Alaska: Effects of climate change on forest insect populations. *Proceedings of the 6th International Conference on Disturbance Dynamics in Boreal Forests* (p. 26).

Wolken, J. M., Hollingsworth, T. N., Rupp, T. S., Chapin, F. S., III, Trainor, S. F., Barrett, T. M., ... Yarie, J. (2011). Evidence and implications of recent and projected climate change in Alaska's forest ecosystems. *Ecosphere*, *2*(11), 124–158.

Zurell, D., Jeltsch, F., Dormann, C. F., & Schroder, B. (2009). Static species distribution models in dynamically changing systems: How good can predictions really be? *Ecography*, *32*, 733–744.